

# NANOTHERANOSTICS

**Overcoming hypoxia-induced chemoresistance to cisplatin through tumor oxygenation monitored by optical imaging**

Donghui Song<sup>a,1</sup>, André O'Reilly Beringhs<sup>a,1</sup>, Zhenwu Zhuang<sup>b</sup>, Gaurav Joshi<sup>a,2</sup>, Thanh Huyen Tran<sup>a,3</sup>, Kevin P. Claffey<sup>c</sup>, Hong Yuan<sup>d</sup>, Xiuling Lu<sup>a\*</sup>

<sup>a</sup>Department of Pharmaceutical Sciences, University of Connecticut, Storrs, Connecticut, USA 06269

<sup>b</sup>Section of Cardiovascular Medicine, Department of Medicine, Yale University School of Medicine, New Haven, CT, USA 06519

<sup>c</sup>Department of Cell Biology, University of Connecticut Health Center, Farmington, Connecticut, USA 06030

<sup>d</sup>Department of Radiology, School of Medicine, University of North Carolina at Chapel Hill, North Carolina, USA 27599

<sup>1</sup>Equal contributors to this work.

\*Corresponding author: Xiuling Lu

xiuling.lu@uconn.edu

University of Connecticut – School of Pharmacy

69 N Eagleville Rd Unit 3092, Storrs, CT USA 06269-3092

## SUPPLEMENTARY DATA

### SUPPLEMENTARY METHODS

#### Chemicals and reagents

Perfluorooctyl bromide (PFOB), L- $\alpha$ -phosphatidylcholine, and cholesterol were purchased from Sigma-Aldrich Corp. (St. Louis, MO, USA). 1,2-distearoyl-sn-glycerol-3-phosphoethanolamine-N-[amino(polyethylene glycol)-2000] ammonium salt (DSPE-PEG 2000 amine) was purchased from Avanti Polar Lipids, Inc. (Alabaster, AL, USA). Polysorbate 60 (Tween<sup>®</sup> 60) was obtained from Croda Health Care (New Castle, DE, USA). Cisplatin (CPT) was purchased from Santa Cruz Biotechnology, Inc. (Santa Cruz, CA, USA). Cell Counting Kit-8 (CCK-8) was obtained from Dojindo Molecular Laboratories, Inc. (Rockville, MD, USA). Hypoxyprobe<sup>™</sup>-1 Plus kit was purchased from Hypoxyprobe, Inc. (Burlington, MA, USA). A549 human lung carcinoma cell line was obtained from the US National Cancer Institute (Frederick, MD, USA). NIR-FLIVO<sup>™</sup>-747 *in vivo* apoptosis assay kit was purchased from ImmunoChemistry Technologies, LLC. (Bloomington, MN, USA). Image-iT<sup>™</sup> Hypoxia Reagent was obtained from ThermoFisher Scientific, Inc. (Waltham, MA, USA). Saline refers to a 0.9% (w/w) sodium chloride solution. All other reagents and solvents were of analytical grade.

#### Preparation of PFOB nanoemulsion

To prepare the 20% (v/v) PFOB nanoemulsion, 26 mg of L- $\alpha$ -phosphatidylcholine, 14 mg of cholesterol and 0.4 mg of DSPE-PEG 2000 amine were dissolved in 2 mL of chloroform. A thin film was formed upon the removal of the solvent by vacuum drying. The film was subsequently hydrated with 1.6 mL of ultrapure water and sonicated in a 65°C water bath for 1 h. This was followed by the addition of 40 mg of Tween<sup>®</sup> 60 and sonication in the 65°C water bath for another 25 min. To this mixture, 400  $\mu$ L of PFOB were added, followed by sonication in an ice bath at an amplitude level of 20% for 10 cycles (2 min per cycle) to allow the complete emulsification of PFOB. The resulting nanoemulsion was filtered through a 0.45  $\mu$ m syringe filter and stored in a sterile glass vial.

#### PFOB nanoemulsion oxygenation

Preformed PFOB nanoemulsions were oxygenated using an in-house apparatus consisting of an air-tight glass vial with two needle accesses. The left 21G needle access (PrecisionGlide<sup>™</sup>, BD, USA) was positioned underneath the PFOB nanoemulsion meniscus and connected to a compressed oxygen tank

(USP grade, Airgas<sup>®</sup>, USA) regulated at 3 L/min gas flow. The right 21G needle access (PrecisionGlide<sup>™</sup>, BD, USA) was positioned near the top of the glass vial and allowed for gas escape and pressure equalization within the glass vial. Oxygen was bubbled for 3 min at a 3 L/min gas flow. Upon ending of oxygenation period, needles were immediately removed, sealing the vial under an oxygen-rich atmosphere. Pre-oxygenated PFOB nanoemulsions (OxyPN) were immediately used in subsequent experimental procedures. A schematic representation of the assembly used for oxygenation via O<sub>2</sub> bubbling is depicted in Figure S1A.

### **PFOB nanoemulsion characterization**

PFOB nanoemulsions were characterized with respect to particle size distribution, zeta potential, PFOB load and encapsulation efficiency, and oxygenation dynamics as described below.

#### ***Particle size and zeta potential distributions***

Samples were diluted in ultra-pure grade water (Milli-Q system, Millipore, USA) at a 1:10 dilution and transferred into clear cuvette. Samples were analyzed via dynamic light scattering using the Zetasizer Nano-ZS instrument (Malvern Instruments Ltd., UK). Analyses were performed at 25°C with a non-invasive backscatter (NIBS) angle of 173°.

Zeta potential distribution was assessed by transferring the diluted sample into folded capillary cells (), which were subsequently analyzed via laser doppler anemometry using the Zetasizer Nano-ZS instrument (Malvern Instruments Ltd., UK) at 25°C.

#### ***PFOB load and encapsulation efficiency***

PFOB load and encapsulation efficiency were determined using a gravimetric method. 250 µL of each formulation was transferred into a centrifuge tube (n=6). Around 100 µL of chloroform was added to the tube and vigorously mixed for 1 h to ensure the solubilization of all formulation's components besides PFOB, which is insoluble and immiscible in chloroform. Tubes were centrifuged for 1 h (relative centrifugal force = 2655 g; 20°C). A tri-phasic dispersion was formed where, based on density, the top layer was the aqueous supernatant (1.0 g/cm<sup>3</sup>), the middle layer was chloroform with phospholipids and cholesterol dissolved in it (~1.49 g/cm<sup>3</sup>), and the bottom one was pure PFOB (1.93 g/cm<sup>3</sup>). The bottom layer was transferred to a clean tube and weighed for the absolute PFOB content. PFOB load was

determined as the volume of PFOB per unit volume of nanoemulsion, and encapsulation efficiency was calculated as the percentage amount of PFOB present in the formulation with respect to the original amount added during manufacturing.

### ***Oxygenation dynamics characterization***

Oxygenation dynamics were assessed via AL300 oxygen sensor probe attached to the NeoFox-GT fluorometer (Ocean Optics, USA). PFOB nanoemulsion (2 mL) was added to a closed vial and assembled for oxygenation as described in “PFOB nanoemulsion oxygenation” subsection. A third needle was added to the system through which the AL300 oxygen sensor probe passed through and reached the formulation on the bottom of the vial (Figure S1B). Oxygenation was performed by bubbling pure O<sub>2</sub> into glass vials containing the PFOB nanoemulsion for up to 3 min. Oxygen levels were allowed to stabilize under hyperoxic environment (closed air-tight vial) for 5 min. Next, *in vitro* oxygen release was simulated upon unsealing the air-tight vial for atmospheric re-equilibration.

The responsiveness of Image-iT<sup>TM</sup> hypoxia optical probe was also verified upon its addition to non-oxygenated and pre-oxygenated PFOB nanoemulsion. Image-iT<sup>TM</sup> probe (5 μL) was mixed with 145 μL of formulation on a 96-well polystyrene plate and immediately imaged using the *In Vivo* Imaging System<sup>®</sup> (IVIS<sup>®</sup>) Lumina LT Series III (excitation = 500 nm, emission = 650 nm, Perkin Elmer, Inc., USA). The radiant efficiency was measured for each well and used to compare the responsiveness of Image-iT<sup>TM</sup> probe to the oxygen level of PFOB nanoemulsion.

### **Cell culture**

A549 cells were cultured in Dulbecco’s Modified Eagle’s Medium (DMEM) supplemented with 10% fetal bovine serum, 1% penicillin/streptomycin, and 1% L-glutamine in a 37°C incubator supplied with 5% CO<sub>2</sub>. A549 cells were conditioned into a hypoxic state by incubating the cells in a sealed hypoxic chamber (MIC-101, Billupus-Rothenberg Inc., USA) containing a gas mixture of 1% O<sub>2</sub> and 5% CO<sub>2</sub> balanced with 94% N<sub>2</sub> at 37°C for 24 h. A549 cells were conditioned into a normoxic state by incubating the cells in 20% O<sub>2</sub> and 5% CO<sub>2</sub> balanced with 94% N<sub>2</sub> at 37°C for 24 h.

### ***In vitro* A549 cytotoxicity**

Hypoxic A549 cells were subsequently treated with 10, 30 or 60  $\mu\text{M}$  CPT followed by incubation for 24 h in ambient air (21%  $\text{O}_2$ ), under carbogen (hyperoxic environment) for 3 h followed by 21 h incubation under ambient air, or with pre-oxygenated 0.4% v/v PFOB nanoemulsion in DMEM with incubation under carbogen as above. Cell viability was assessed by adding a solution containing 10  $\mu\text{L}$  of CCK-8 and 100  $\mu\text{L}$  of fresh cell culture medium to each well after incubation. Cells were then incubated for an additional 2 h at 37°C under 5%  $\text{CO}_2$ . Finally, absorbance values were measured at 450 nm using a microplate reader. Cells treated with saline and cultured under similar conditions were used as negative controls for each group.

### **Animals and human lung cancer xenograft tumor model**

Severe combined immunodeficiency (SCID) mice were purchased from the Jackson Laboratory (Farmington, CT, USA) and housed in a pathogen-free animal facility at the University of Connecticut, School of Pharmacy. All animal experiments were conducted in accordance with regulations and guidelines of the Institutional Animal Care and Use Committee (protocol A14-046). For the xenograft lung tumor model, A549 cells ( $2 \times 10^6$ ) suspended in 100  $\mu\text{L}$  of PBS buffer were subcutaneously injected into the right flanks of 6-8 week-old mice.

### ***In vivo* optical imaging of real-time oxygenation level in tumor**

Fifty  $\mu\text{L}$  of a 1 mM Image-iT<sup>TM</sup> hypoxia reagent solution in DMSO was intratumorally injected to tumors averaging 75  $\text{mm}^3$ , and the fluorescence signals monitored using the In Vivo Imaging System<sup>®</sup> (IVIS<sup>®</sup>) Lumina LT Series III (Perkin Elmer, Inc., USA) at excitation and emission wavelengths of 500 and 650 nm, respectively. Twelve hours post administration, tumor fluorescence signals reached steady-state and the animals were divided into 4 treatment groups (5 mice per group): (1) OxySaline+ $\text{O}_2$ : mice administered intravenously with 50  $\mu\text{L}$  of pre-oxygenated saline (0.9% NaCl) and allowed to breath carbogen (95%  $\text{O}_2$  and 5%  $\text{CO}_2$ ); (2) OxyPN+ $\text{O}_2$ : mice administered intravenously with 50  $\mu\text{L}$  of pre-oxygenated PFOB nanoemulsion, and then allowed to breath carbogen; (3) PN+ $\text{O}_2$ : mice administered intravenously with 50  $\mu\text{L}$  of non-oxygenated PFOB nanoemulsion, and then allowed to breath carbogen; and (4) OxyPN+Air: mice administered intravenously with 50  $\mu\text{L}$  of pre-oxygenated PFOB nanoemulsion, then kept in ambient air (21%  $\text{O}_2$ ). The content of PFOB in the nanoemulsion used was 20% (v/v). Fluorescence signals were monitored at 5 and 20 min, 1, 2, 3, 4, 5, and 6 h post-treatment.

Quantification was conducted by measuring the fluorescence intensity (average radiant efficiency) in the region of interest (ROI).

To assess the impact of tumor oxygenation from circulating PN and PN accumulated in tumor tissue, mice were administered with OxyPN or saline and 24 h later the animals received an intratumoral dose of Image-iT™ hypoxia reagent. Fluorescence signal was allowed to stabilize for 3 h and background signal was measured (27 h post initial treatment). Animals were allowed to breath carbogen (95% O<sub>2</sub> and 5% CO<sub>2</sub>) for 1 h and re-imaged to assess the oxygenation effect attributed to lingering PN in blood circulation at 28 hours post injection.

### ***Ex vivo* optical imaging of apoptosis in tumors**

Tumor apoptosis was evaluated *in vivo* by comparing three groups of tumor-bearing SCID mice (n=3): (1) intravenous administration of 5 mg/kg of CPT with ambient air breathing for 3 h; (2) intravenous administration of 5 mg/kg of CPT with carbogen breathing for 3 h; and (3) intravenous administration of 5 mg/kg of CPT in pre-oxygenated 20% (v/v) PFOB nanoemulsion (50 μL i.v. injection) with carbogen breathing for 3 h. Forty-eight hours post treatment, the NIR-FLIVO™-747 *in vivo* apoptosis assay agent was intravenously administered to the mice (50 μL via tail vein; 1x NIR-FLIVO™ solution per mouse). Four hours post NIR-FLIVO™-747 injection, tumors were excised from mice and imaged using the IVIS® Lumina LT Series III (Perkin Elmer, Inc., USA) at excitation and emission wavelengths of 747 and 776 nm, respectively.

### ***In vivo* antitumor efficacy & *ex vivo* apoptosis staining**

Tumor-bearing mice with average tumor sizes of 60-75 mm<sup>3</sup> were randomly assigned to 5 different groups (n=4) for subsequent treatment. Mice were administered intravenously with 50 μL of (1) saline; (2) CPT: free cisplatin (1 mg/kg); (3) CPT+O<sub>2</sub>: free cisplatin (1 mg/kg) under hyperoxic breathing; (4) OxyPN+O<sub>2</sub>: pre-oxygenated PFOB nanoemulsion (20% v/v); or (5) CPT+OxyPN+O<sub>2</sub>: mixture of cisplatin and pre-oxygenated PFOB nanoemulsion (20% v/v), where the cisplatin dose was 1 mg/kg. All treatments were administered once per week for up to 40 days. Mice subjected to hyperoxic breathing were kept in a carbogen-filled chamber (95% O<sub>2</sub> and 5% CO<sub>2</sub>) for 3 h post-injection. Remaining mice were allowed to breathe ambient air. Tumor volumes were measured every three days using a caliper

and calculated as:  $V (mm^3) = \frac{1}{2} \times length \times width^2$ . The relative change in tumor volume was calculated using the  $V/V_0$  ratio where  $V_0$  is the initial tumor volume.

At the end of the study, animals were euthanized, and tumors were harvested. Tumors were blocked in paraffin and sectioned into 5  $\mu$ m-thick slices. Slices were stained with hematoxylin and eosin (H&E). Terminal deoxynucleotidyl transferase (TdT) dUTP nick-end labeling (TUNEL) staining was also performed as means to detect DNA fragmentation for apoptosis assessment. Representative slices of each group were analyzed under an optical microscope and the number of apoptotic cells as a percentage of total cells in the HPF was determined (n=4, 10 HPF/tumor).

### ***In vivo* circulation half-life**

Mice were administered intravenously with 50  $\mu$ L of OxyPN and dynamic changes in X-ray attenuation were monitored using the eXplore CT120 system (GE Healthcare, USA) at an 80 kV accelerating voltage. X-ray attenuation was calculated as a function of Hounsfield Units (HU) at the left ventricle.

### ***In vivo* tumor accumulation**

PN was manufactured with the addition of DiR' dye (Dil C<sub>18</sub>(7); Thermo Fisher Scientific, USA) to the lipid solution prior to organic solvent evaporation. Formulation was prepared as described in the "Preparation of PFOB nanoemulsion" subsection. Tumor-bearing SCID mice (average tumor size = 75 mm<sup>3</sup>) were dosed with 50  $\mu$ L of DiR'-loaded PN intravenously (tail vein injection) and fluorescence signals were monitored at 1, 3, 6 and 24 h post-administration. Data collection was performed using the IVIS<sup>®</sup> Lumina LT Series III pre-clinical imaging system (Perkin Elmer, Inc., USA) at excitation and emission wavelengths of 750 and 780 nm, respectively.

### **Histopathological evaluation of toxicity**

At the end of the efficacy study, organs (lungs, spleens, hearts, livers, and kidneys) were harvested, blocked in paraffin and sectioned into 5  $\mu$ m-thick slices, followed by H&E staining. An additional tumor-bearing mouse group was treated with a high dose of CPT (2 mg/kg) to be used as positive control, where toxicity is expected to occur. Histopathological analysis was performed at the Connecticut Veterinary Medical Diagnostic Laboratory by a single-blinded Doctor of Veterinary Medicine.

## **Statistical analysis**

To statistically demonstrate significant differences between groups in related studies, one-way or two-way analysis of variance (ANOVA) tests were performed. Post-hoc analysis was done using Tukey's Multiple Comparison test, unless stated otherwise. Statistical tests were performed using Prism 8.0 software (GraphPad Software Inc., USA).

## **SUPPLEMENTARY RESULTS AND DISCUSSION**

### **PFOB nanoemulsion formation**

PFOB nanoemulsions were prepared yielding homogeneous opaque formulations. Upon PFOB addition to an aqueous dispersion containing phospholipids, it does not mix. However, inputting high sonic energy promotes the dispersion of PFOB droplets in the continuous aqueous phase. Due to the amphiphilic behavior of phosphatidylcholine (surfactant used in our formulation), it interacts with the PFOB droplets, coating their surface, while still interacting with the aqueous environment – thus stabilizing the PFOB nanodroplets.

### ***In vitro* PFOB nanoemulsion oxygenation**

Upon oxygenation for 3 minutes with oxygen bubbling (Figure 1E), dissolved oxygen content in saline increased from  $15.1 \pm 2.4$  ppm to  $136.4 \pm 48.2$  ppm ( $p < 0.0001$ ), whereas PN showed an increase from  $73.7 \pm 8.6$  ppm to  $325.2 \pm 86.4$  ppm ( $p < 0.0001$ ). Oxygen bubbling led to a supersaturated state with respect to the dissolved oxygen content. As soon as oxygen bubbling ceased, the oxygen content quickly reduces. During the period of oxygenation, there is a clear increase in oxygen content in the sample. The high variability observed during oxygen bubbling is likely due to the interference of the bubbles on the fluorometer signal. Upon cessation of bubbling, saline and PN showed a high variation in readings from the fluorometer due to the hyperoxic environment. PN showed enhanced capability of carrying oxygen when compared with saline, leading to a comparative 2.5-fold increase in dissolved oxygen ( $p < 0.0001$ ). The supersaturated oxygen levels are sustained under hyperoxic environment, translating into a metastable condition. Upon opening of the air-tight vial, the hyperoxic headspace quickly equilibrates with the room air (~21% O<sub>2</sub>) and promotes oxygen release from the supersaturated liquid, quickly donating oxygen to the atmosphere following Henry's gas law (Figure S1C). The oxygen contents rapidly decreased for both samples, within a 5 minutes interval. The rate of decrease is apparently

similar for both systems.

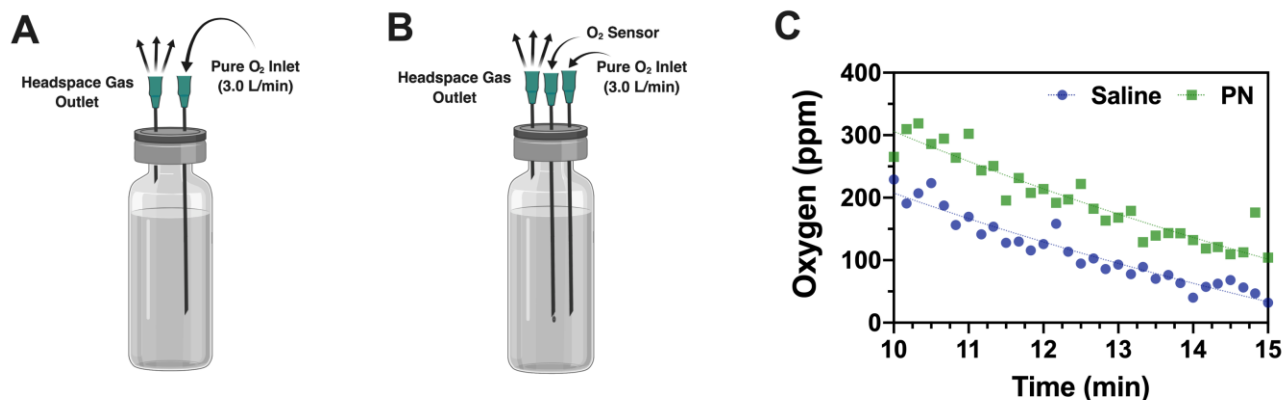


**Figure S1.** (A) Schematic representation of the apparatus used for PFOB nanoemulsion oxygenation, comprised of an air-tight vial, O<sub>2</sub> inlet and headspace gas outlet. (B) Schematic representation of the modified apparatus represented in (A) with a third access for the O<sub>2</sub> fluorometer probe. (C) *In vitro* oxygen release from saturated saline and PN upon loss of hyperoxic atmosphere. Illustrations (A) and (B) were made with BioRender.

### Half-Life of PFOB nanoemulsion

The circulation time of the PFOB nanoemulsion is of utmost importance considering it supplies supplementary oxygen only while in circulation. Additionally, PFOB shows high X-ray attenuation, and therefore it can be directly tracked *in vivo* using X-ray Computed Tomography (CT). Animals were injected with PFOB intravenously (tail vein injection; 50  $\mu$ L/mouse) and the X-ray attenuation as measured in 4 distinct anatomies of interest: right ventricle, left ventricle, aorta and inferior vena cava.

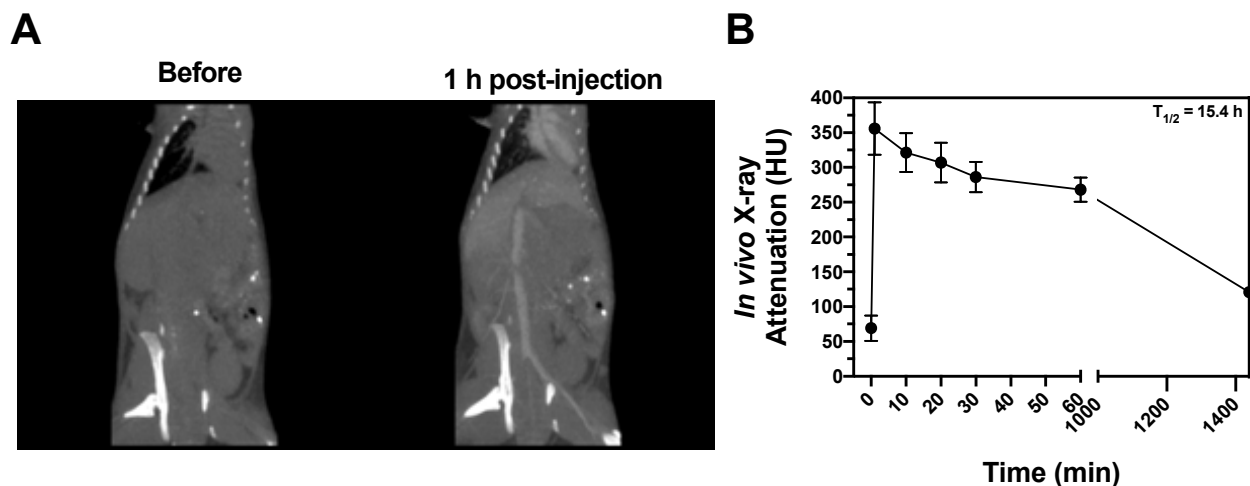


**Figure S2. PFOB nanoemulsion half-life in circulation.** (A) Representative X-ray Computed Tomography sections of a mouse intravenously injected with PFOB nanoemulsion before and one-hour post-injection. (B) X-ray attenuation in heart *versus* time.

Figure S2 summarizes the data collected. A one-compartment intravenous bolus model was applied to the dataset and the half-life of the formulation in circulation (as a function of X-ray attenuation) was measured as 15.4 h, following a rate constant of elimination of  $0.045 \text{ h}^{-1}$ .

### ***In vivo* real-time monitoring of tumor oxygenation levels during PFOB treatment**

Tumors exhibited a certain fluorescence signal due to their inherent hypoxic state upon Image-iT<sup>TM</sup> injection. The fluorescence signal became steady 12 h post administration. The total fluorescence intensity of each tumor at 12 h was set as baseline, representing the hypoxic state prior to PFOB nanoemulsion treatment, and signals at other time points were normalized as percent change with respect to the baseline.

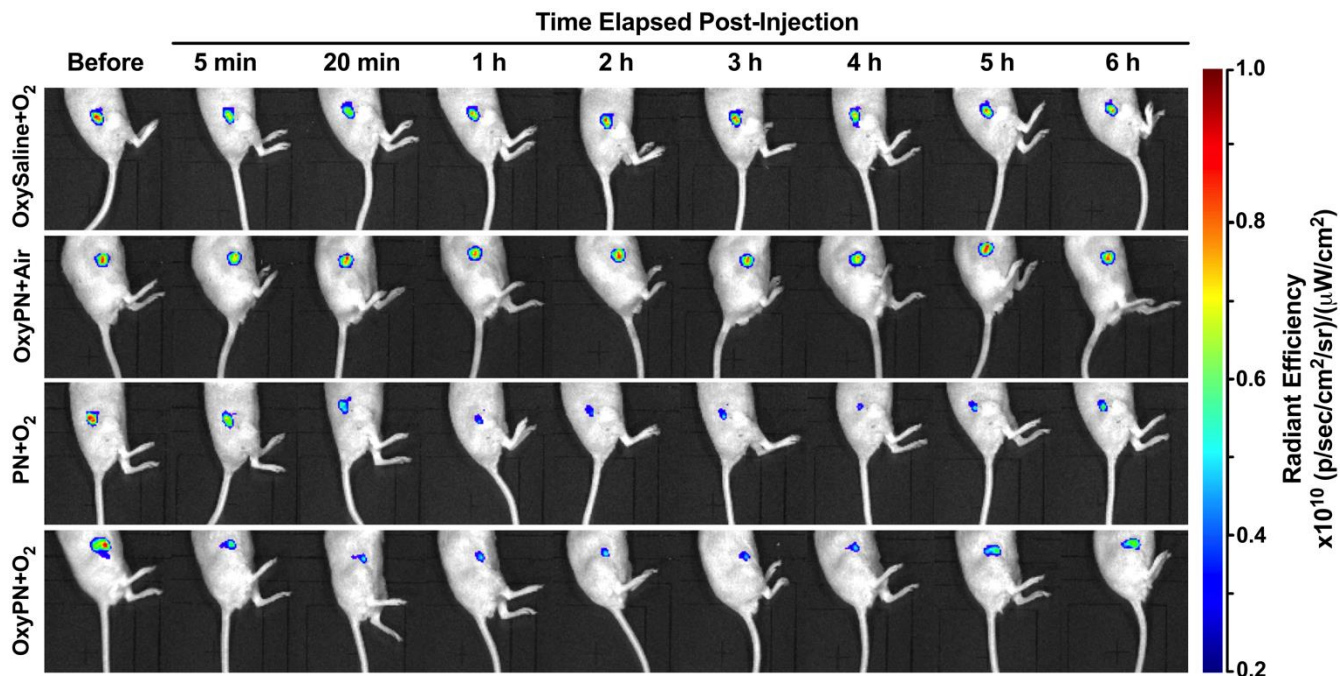


**Figure S3. *In vivo* serial optical imaging of hypoxia in tumors.** Representative images of fluorescence from tumors at all time-points.

Significant signal reduction was observed 5 min post-injection of the pre-oxygenated PFOB nanoemulsion followed by hyperoxic breathing (OxyPN+O<sub>2</sub>; Figure S3). The rapid reduction in fluorescence signal indicated effective and rapid oxygen delivery to tumor tissues after injection. The normalized fluorescence intensity for OxyPN and PN were  $62.8 \pm 4.1\%$  and  $83.5 \pm 12.8\%$  respectively, which translates into a statistically-significant difference ( $p = 0.0077$ ; Two-way ANOVA and Tukey's Multiple Comparison Test). Later time-points did not show differences between OxyPN and PN groups ( $p > 0.05$ ). For the mice treated with the PFOB nanoemulsion without pre-oxygenation under hyperoxic breathing (PN+O<sub>2</sub>), the signal reduced gradually and reached a plateau in one hour. The signal started increasing approximately 4 h post treatment, although the animals were still under the hyperoxic breathing regimen.

### **Reduced CPT off-target toxicity following co-treatment with PFOB nanoemulsion**

General toxicity upon treatment was investigated by monitoring the mice's weight variations throughout the efficacy study. Figure S4 displays relative growth curves for all treated groups. Saline group displayed a growth curve consistent with the natural growth of the animals. This effect was also verified for the OxyPN+O<sub>2</sub> group showcasing the apparent safety of the formulation tested. CPT, CPT+O<sub>2</sub> and CPT+OxyPN+O<sub>2</sub> groups showed reduction in growth rate with respect to saline control, which was due to the known toxicity of cisplatin.

On the histopathological analysis, no signs of oxygen-related toxicity (e.g. lung injury) were observed. No other signs of toxicity were observed in other organs as neither CPT nor the PFOB nanoemulsion caused histological damage to those tissues (Figure S5). These findings sustain the hypothesis that the PFOB nanoemulsion itself did not imply in significant *in vivo* toxicity. Moreover, the reduction in animal growth rate observed *in vivo* was associated solely to the administration of cisplatin and it is an anticipated side-effect of chemotherapy.

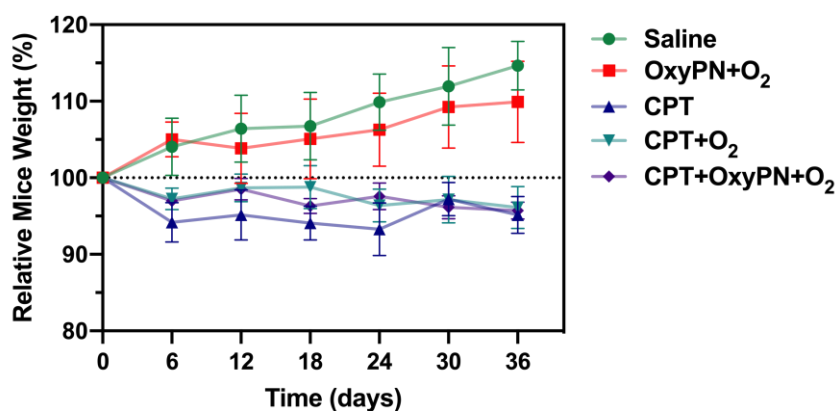


**Figure S4. Relative mice growth curves for treatment groups subjected to the efficacy study with respect to the initial body weight.**

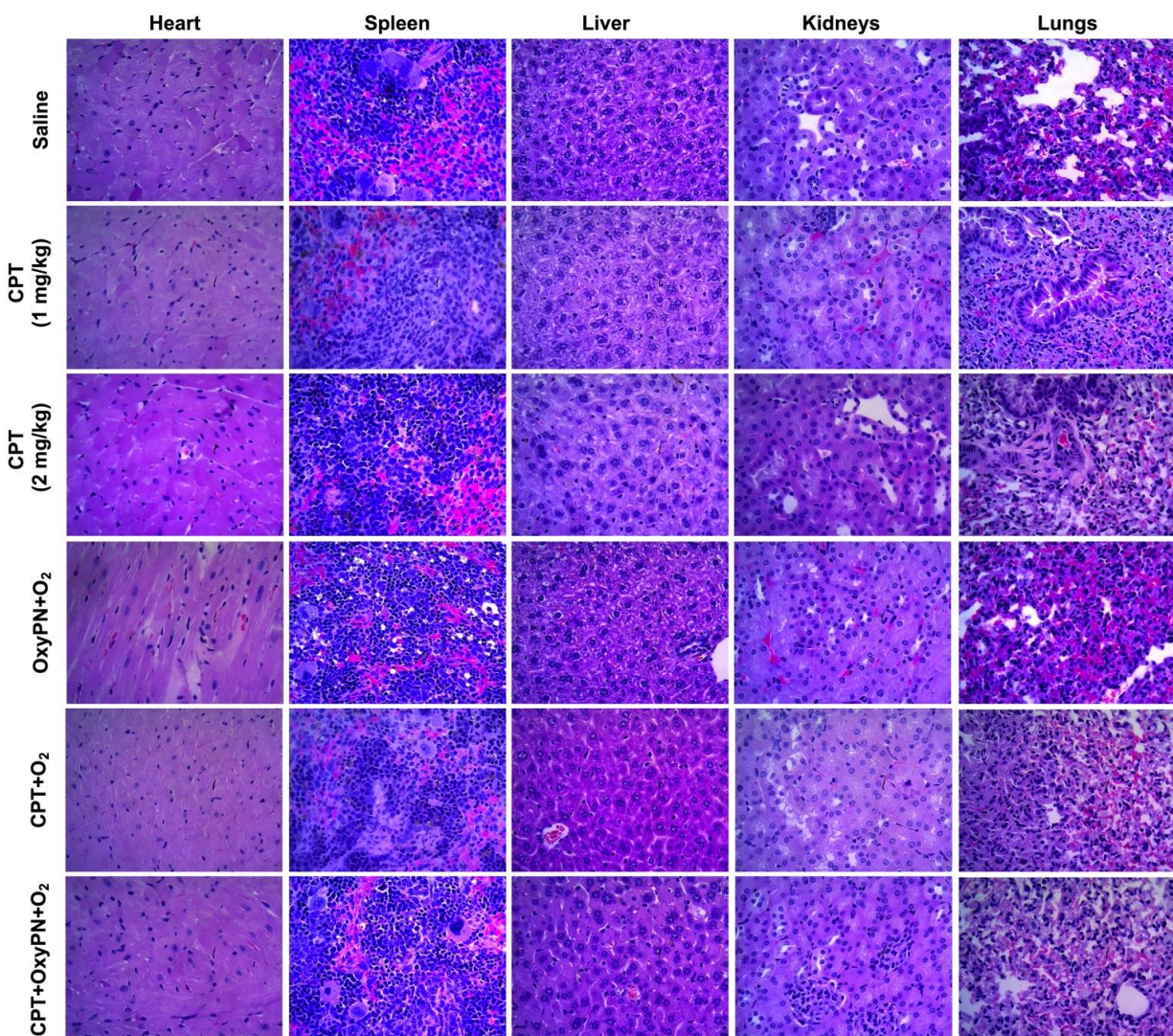


**Figure S5. Histopathological analysis of major organs harvested from treated mice.**

### **Tumor accumulation of PFOB nanoemulsion upon intravenous administration**

PN selective accumulation in tumor tissues was confirmed by preparing a DiR'-labeled PN and administering intravenously to tumor-bearing mice. Animals were tracked for up to 24 h and the fluorescence signal from tumor tissues monitored using an *in vivo* imaging system. Figure S6 displays representative images collected during the experiment.

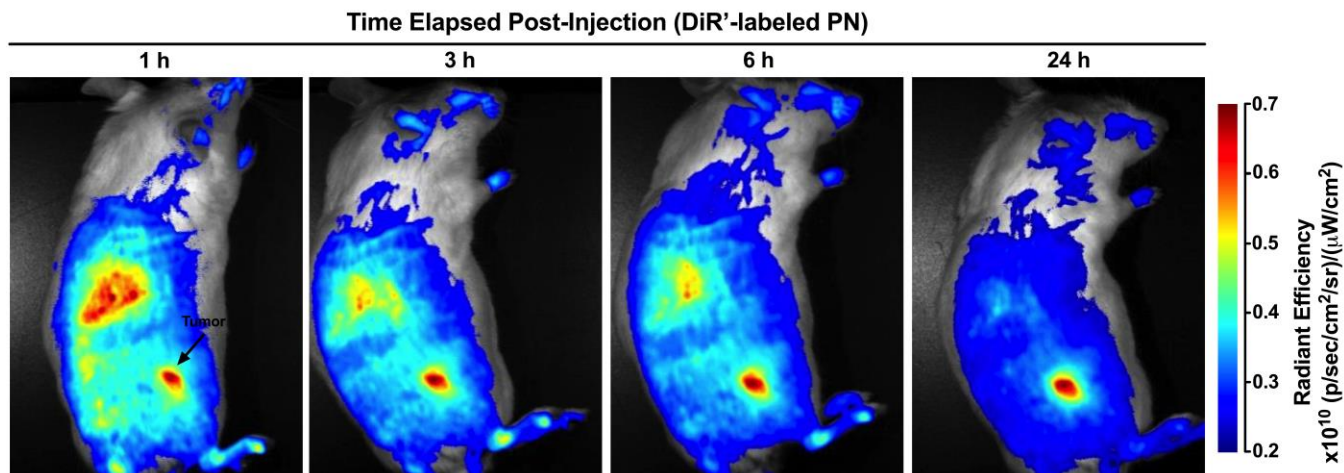


**Figure S6. Tumor accumulation of PFOB nanoemulsion.** Representative fluorescence whole-body images of tumor-bearing mouse injected intravenously with DiR'-labeled PFOB nanoemulsion.

The intravenous administration of DiR'-labeled PN led to an overall increase in background signal in the animal due to the circulating dye. The background signals decreased steadily overtime as PN droplets are removed from the body circulation. Tumor accumulation increased steadily from the first time-point (1 h post-injection) to 6 h post-injection. Tumor signals increased at 24 h but not proportionally, indicating most of the formulation accumulates in tumor tissues at early time-points. Fluorescence signal from liver corroborates these findings as it reaches its maximum at the first time-point due to the vast removal of nanodroplets from circulation. Fluorescence signal in liver reduces steadily as there is less droplets available for removal as time moves forward. These findings are consistent with the pharmacokinetic study of the formulation (Figure S2), as half of the formulation is cleared from blood circulation at approximately 15 h post-administration.